

Det Kongelige Danske Videnskabernes Selskab

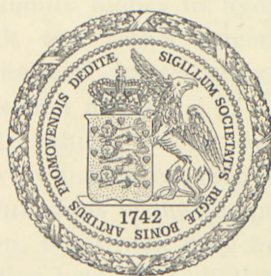
Matematisk-fysiske Meddelelser, bind **26**, nr. 5

Dan. Mat. Fys. Medd. **26**, no. 5 (1951)

THE TOTAL CHARGES  
OF FISSION FRAGMENTS IN  
GASEOUS AND SOLID  
STOPPING MEDIA

BY

N. O. LASSEN



København

i kommission hos Ejnar Munksgaard

1951

THE SCIENTIFIC JOURNAL OF THE ROYAL DANISH ACADEMY OF SCIENCES

Published by the Royal Danish Academy of Sciences, Copenhagen, Denmark.

Volume 10, No. 1, 1911.

# ON THE THEORY OF THE CHANGES IN THE POSITION OF THE EQUATOR AND THE POLAR AXIS

By *Dr. P. G. LEVY*, *Professor of Mathematics at the University of Copenhagen.*

Received for publication on the 15th of October 1910.



Printed in Denmark.  
Bianco Lunos Bogtrykkeri.

## Introduction.

Some years ago the total charges of fission fragments leaving a uranium surface were determined by measurements of the curvature of the paths which were described by the fragments in the magnetic field of the cyclotron. The most frequent values of the charges were found to be  $20$  and  $22\epsilon$  for the light and heavy fragment, respectively<sup>(1,2)</sup>. Later, the specific ionization by the fragments along the range was measured in several gases<sup>(3, 4, 5)</sup>. From the latter measurements the effective charges were calculated by means of the stopping formula given by BOHR<sup>(6)</sup>. They were found to have absolute values agreeing quite well with the observed total charges, but the light fragment was found to have the higher effective charge in contrast to the result of the deflection measurements, which clearly showed that it has the lower total charge. From the values of the specific ionization it was indicated that the effective charge of the light fragment might be slightly higher in hydrogen than in heavier gases, but this result was rather uncertain. It was therefore decided to measure the total charges in hydrogen and other gases by means of the deflection method.

These experiments, which will be described in the present paper, have yielded very interesting results<sup>1</sup>. It is found that the charges in gases are functions of the gas pressure, a result which had not been foreseen, but which may be readily explained as a result of a competition between radiation and loss of electrons from excited states in the fragment ions. At least at low pressures the charges are much smaller than the charges in solid materials, a fact which enables us to estimate the order of magnitude of the

<sup>1</sup> A short account of the main results was given in a recent note in *The Physical Review*(7).

cross-section for electron capture by the fragments in gases. Furthermore, the experiments show that in gases the light fragment has a higher charge than the heavy fragment opposite to what is the case in solids, removing in this respect the discrepancy between the effective and the total charges.

In the following a short description of the experimental technique will be given in Chapter I. In Chapter II the results obtained in gases at low pressure will be presented; Chapter III deals with a few measurements of the charges in solids, and Chapter IV with the measurements in gases at higher pressures leading to the variation of the charges with pressure.

## Chapter I. Experimental Technique.

### § 1. Apparatus.

In Fig. 1 (1) denotes the brass wall of the acceleration chamber of the cyclotron. (2) is a stud consisting of a 3-inch copper tube and a flange, on which the actual deflection apparatus is mounted. The apparatus consists of two chambers; the inner chamber, which may be called the deflection chamber, is limited by a brass disk (3), a 5-inch copper tube (4), a flange (5), a 3-inch brass tube (6), a brass plate (7), and a copper pyramid (8). Outside the top of the pyramid four cooling tubes run, to which a beryllium plate (9) is soldered. (10) indicates the position of the Dees and the figure furthermore indicates an 8-MeV deuteron beam hitting the beryllium plate, which thus acts as a strong neutron source. Inside the pyramid, close to the top a mica sheet (11) carrying a uranium layer is placed; the layer is made by evaporation *in vacuo* in a special chamber. (12) is a slit made by two brass knives held by the brass plate (13), which is supported on a movable slide (not shown in the figure) and can be operated from outside by means of the rod (14), against which it is pressed by a spring. The bellow (15) permits the rod to be moved about 25 mm in a direction along its axis; the position of the rod and therefore of the slit can be read on an outside scale with an accuracy of 0.1 mm.

In the brass disk (3) is cut a second slit (16), but this slit is covered by a thin mica foil fastened to the disk by means of

apiezon wax, so that no gas can penetrate into the deflection chamber from the second chamber. This outer chamber is made

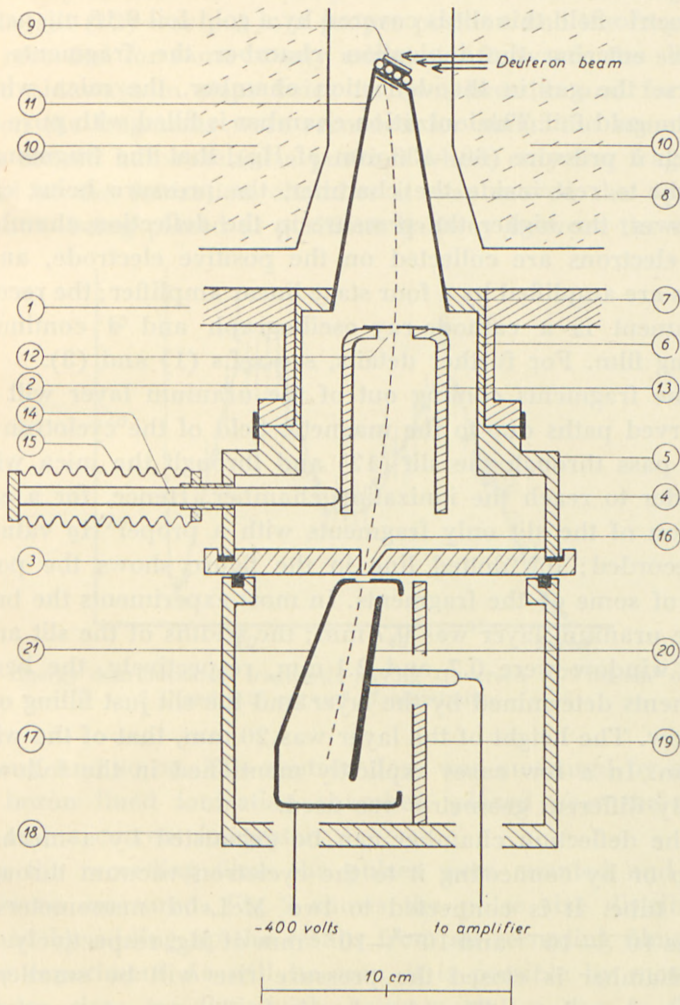


Fig. 1. Experimental apparatus.

of a 5-inch copper tube (17) and a brass plate (18); it contains an ionization chamber, the two electrodes of which are mounted on the brass plate (19) by means of insulating supports (not shown). One of the electrodes (20) is simply a brass plate, while

the second electrode (21) is formed as a box surrounding the former. The fission fragments enter the ionization chamber through a slit in the second electrode; in order not to destroy the electric field this slit is covered by a gold foil 0.18 mg per cm<sup>2</sup>. Before entering the ionization chamber the fragments must traverse the gas in the deflection chamber, the mica window, and the gold foil. The ionization chamber is filled with pure argon to such a pressure (60—130 mm of Hg), that the fragments are brought to rest inside the chamber, the pressure being chosen the lower, the higher the pressure in the deflection chamber is. Free electrons are collected on the positive electrode, and the pulses are amplified by a four stage linear amplifier; the recording instrument is a cathode-ray oscillograph and a continuously moving film. For further details, see ref.s (1) and (3).

The fragments coming out of the uranium layer will move in curved paths due to the magnetic field of the cyclotron; they must pass through the slit (12) and through the mica window in order to reach the ionization chamber. Hence, for a certain position of the slit only fragments with a proper  $Hq$  value will be recorded; the dotted line in the figure shows the possible path of some of the fragments. In most experiments the breadth of the uranium layer was 0.7 mm; the widths of the slit and the mica window were 0.7 and 2.1 mm, respectively, the beam of fragments determined by the layer and the slit just filling out the window. The height of the layer was 20 mm, that of the window 60 mm. In a few cases explicitly mentioned in the following a slightly different geometry was used.

The deflection chamber can be exhausted by a mechanical pump or by connecting it to the cyclotron vacuum through an outer tube. It is connected to two McLeod manometers with ranges  $10^{-4}$ — $10^{-1}$  and  $10^{-2}$ — $10^{+2}$  mm of Hg, respectively. When the chamber is closed the pressure rise will be smaller than  $10^{-3}$  mm per hour. The chamber is furthermore connected to a glass tube which during all experiments were cooled in liquid air, except the experiments with xenon, in which the liquid air was replaced by solid carbon dioxide in alcohol.

## § 2. General procedure.

The experiments were usually carried out in the following way:

The slit (12) was put in a proper position and the fragments were recorded for some twenty minutes. Afterwards the slit was moved sideways in steps twice its own breadth and for each position the fragments were recorded for about the same time. When the slit had reached a position where only few fragments arrived at the ionization chamber it was moved the opposite way, now being placed at positions halfway between the earlier

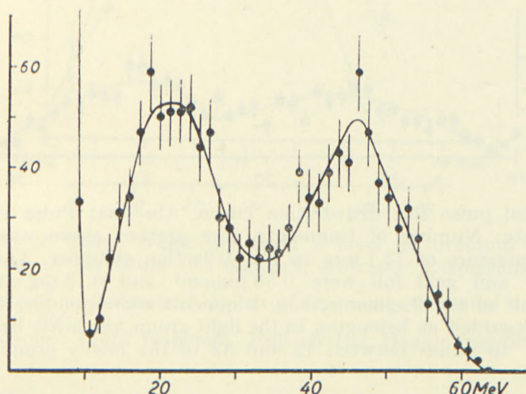


Fig. 2. Energy distribution of fragments having traversed  $0.79 \text{ mg/cm}^2$  of mica and  $0.25 \text{ mg/cm}^2$  of aluminum.

positions, and so on. The neutron dose was measured by means of a boron lined ionization chamber, placed near the cyclotron, and a current integrater.

On the recording films the pulses were counted and their sizes were measured. Fig. 2 shows the pulse size distribution obtained by adding up the results from all recording films in a certain experiment. As will be seen, it is possible by means of the pulse sizes to distinguish between pulses due to fission fragments and to background caused by  $\gamma$ -rays and neutrons. Furthermore, the two groups of fragments can be roughly separated from each other by identifying fragments of sizes higher or lower than 34 MeV with the light or the heavy group, respectively.

The distribution in Fig. 2 was obtained with a 1 mm uranium layer, a 1 mm slit, and a 3 mm window; the uranium layer was

rather thin ( $\approx 0.2 \text{ mg/cm}^2$ ) and it was mounted in a way slightly different from that shown in Fig. 1 so that the observed fragments were emitted normally from the surface. In most of the experiments, where uranium layer and slit were only 0.7 mm and the window 2 mm, the layer was chosen much thicker ( $0.6\text{--}0.8 \text{ mg/cm}^2$ ) and it was placed in the way shown in order to give a sufficient yield. The fragments reaching the ionization chamber traversed the layer obliquely, the paths making angles of about  $45^\circ$  with the normal. For these reason the spread in pulse sizes was somewhat greater and the valley between the two peaks

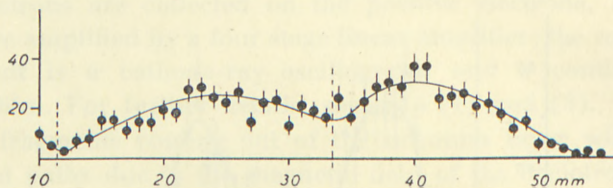


Fig. 3. Typical pulse size distribution curve. Abscissa: Pulse size in arbitrary units. Ordinate: Number of fragments. The present curve was obtained with helium at a pressure of 12.1 mm in the deflection chamber. The thicknesses of mica window and gold foil were  $0.58 \text{ mg/cm}^2$  and  $0.18 \text{ mg/cm}^2$ , respectively. The upper half of the fragments, e. g. fragments corresponding to pulses higher than 33 are regarded as belonging to the light group, the lower half corresponding to pulses between 12 and 32 to the heavy group.

on the distribution curve was not so deep. Consequently, the dividing line between the two groups was not very well-defined and, hence, in stead of using the curve to determine this line, it was simply obtained by dividing the total number of fragments into two equal parts. Fig. 3 shows a typical pulse size distribution curve.

The results of the counting were plotted in a diagram giving the number of fragments as a function of the displacement of the slit. As an example the distribution of the deflection of fragments having passed a thin layer of beryllium is shown in Fig. 4. From the diagram the most frequent deflection values for the light and heavy fragment are found to be  $13.0 \pm 0.3$  and  $13.9 \pm 0.3 \text{ mm}$ , respectively. The deflection as measured by the displacement  $a$  of the slit is proportional to  $\frac{e}{mv}^{(1)}$ , and since  $mv$  does not vary much among the fragments (about  $\pm 10$  per cent. from the mean value<sup>(1)</sup>) and is the same for both groups of fragments, the distribution curve gives a rough picture of the charge



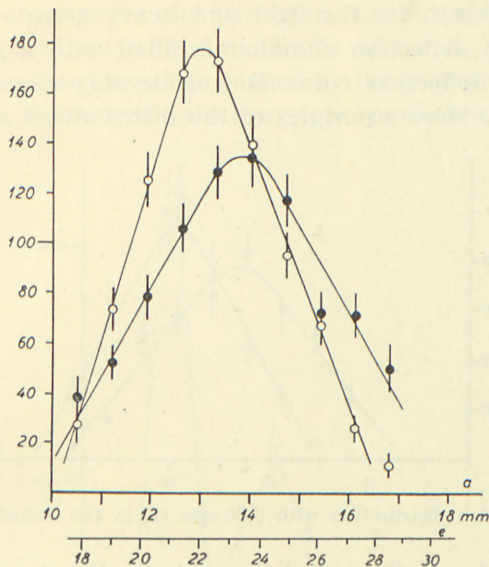


Fig. 4. Deflection of fission fragments from a layer of uranium ( $0.7 \text{ mg/cm}^2$ ) covered by a layer of beryllium ( $0.1 \text{ mg/cm}^2$ ). Abscissa: Displacement  $a$  of slit in mm.  $a = \text{const.} \times \frac{e}{mv}$ . Ordinate: Number of fragments for equal neutron doses. Open circles: Light fragment. Full circles: Heavy fragment.

distribution. The scale, given by  $e = 1.7 \times a$ , is shown in the figure; it has been calculated from the known magnetic field and its variation along the radius of the cyclotron and was checked by means of  $ThC'$   $\alpha$ -particles in the same way as in the earlier experiments<sup>(1)</sup>. The scale is not the same as earlier, because the magnetic field is about 20 per cent. higher, the cyclotron now being operated at a higher deuteron energy. The most frequent charges are found to be 22 and  $23.5 \epsilon$  for the light and heavy fragment, respectively.

## Chapter II. Results in Gases at Low Pressure.

### § 1. General remarks.

The deflection distribution obtained from uncovered uranium with vacuum in the deflection chamber ( $p \approx 10^{-3} \text{ mm}$ ) is similar to that shown in Fig. 4; the peaks lie at displacement values

11.8 and 13.0 mm for the light and heavy group, respectively. But when the deflection chamber is filled with a gas to a low pressure the deflection curve is considerably changed. Figs. 5, 6, 7, 8, and 9 show examples of the distributions obtained; the

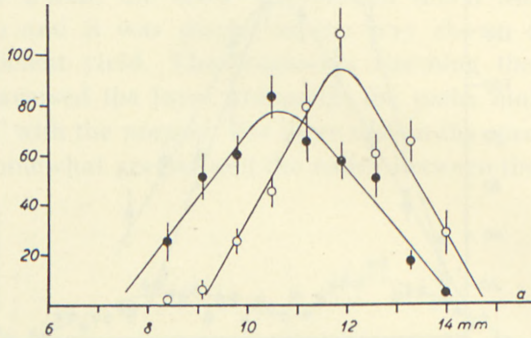


Fig. 5. Deflection distribution with 0.06 mm H<sub>2</sub> in the deflection chamber.

differences between these and the curve in Fig. 4 are rather outstanding.

Firstly, the light fragment suffers higher deflection than the heavy fragment, which means that in gases the former has the

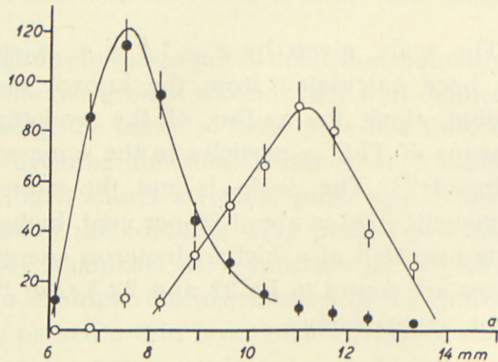


Fig. 6. Deflection distribution with 0.67 mm H<sub>2</sub> in the deflection chamber.

higher charge, opposite to what is the case in uranium, as was already mentioned in the Introduction.

Secondly, at not too low pressures the deflection curves are much narrower than those shown in Fig. 4. On the figures it may be followed, how the width of the curves decreases with increasing pressure; a minimum width is reached for pressures of

about 1 mm argon or 10 mm hydrogen, and for higher pressures the width is constant within the limits of error. This width is slightly greater than the width caused by the geometrical arrangement. As seen, the curve for the heavy group reaches the minimum

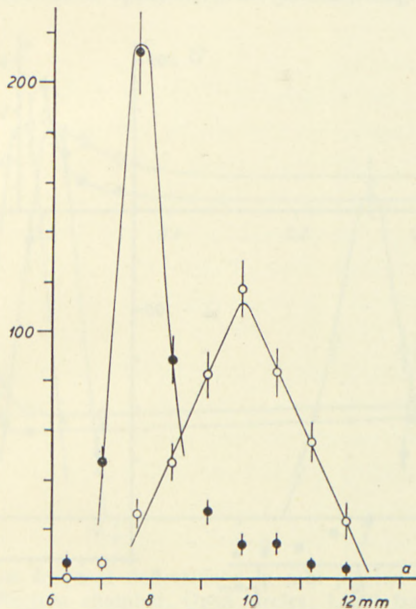


Fig. 7. Deflection distribution with 3.8 mm  $H_2$  in the deflection chamber.

width for a lower pressure than does the curve for the light group.

The difference between the widths found with vacuum and with a gas in the deflection chamber may be understood by the following considerations. Suppose for a moment that we had a homogeneous group of fragments with definite values of  $m$ ,  $v$ , and  $z$ , and that the geometry were infinitely good. Since the charge  $e$  is determined by a balance between capture and loss of electrons, it will not be constant along the path, but fluctuations of one or more electronic charges will occur. But when the pressure in the deflection chamber is sufficiently high, so that many interchanges of charge take place along the path traversed inside the chamber, the deflections will be determined merely by the mean charge, and the fluctuations will have no influence on

the shape of the deflection curve. However, for  $p = 0$ , when no interchanges of charge takes place in the deflection chamber, the charge distribution at a definite point of the range will be obtained; this distribution is determined by the number of possible  $e$ -values and the probability with which they occur. Hence, for

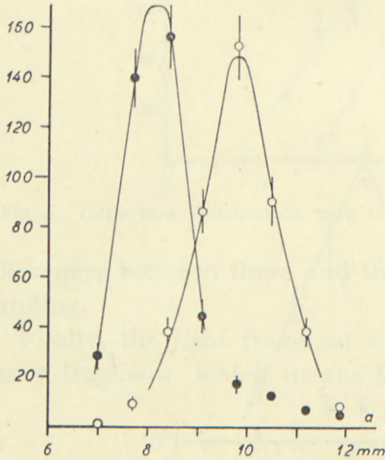


Fig. 8.

Fig. 8. Deflection distribution with 10.7 mm  $H_2$  in the deflection chamber.

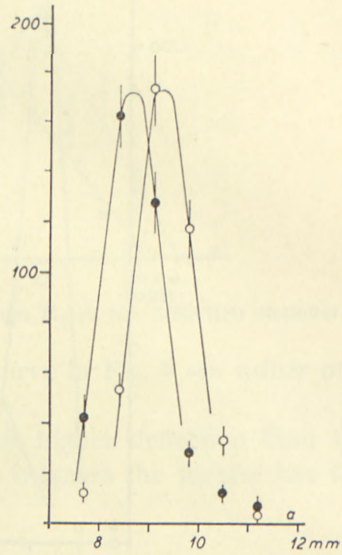


Fig. 9.

Fig. 9. Deflection distribution with 0.9 mm A in the deflection chamber.

reasonably high pressures we shall expect the curves to be sharp, while for  $p = 0$  they give the distribution of the charges of fragments emerging from solids. The fragments are not homogeneous, and the geometry is rather imperfect, and for both reasons the curves are considerably broadened; nevertheless, since the difference between the curves is so large, the curves for  $p = 0$  may be taken as a rather good picture of the charge distribution caused by the fluctuations.

A third difference between the curves in Fig. 4 and those in the following figures is, that the absolute values of the charges are much smaller for higher pressures than for  $p = 0$ . As seen from Figs. 5—9 the deflection decreases with increasing pressure more strongly for the heavy than for the light fragment. This is more

clearly seen from Fig. 10, which gives the most frequent values of the deflection  $a$ , as obtained from the deflection curves, plotted against the pressure of argon in the deflection chamber. As already mentioned,  $a$  is approximately proportional to  $e$ ; the velocity decrease for a pressure of 4 mm argon is about two

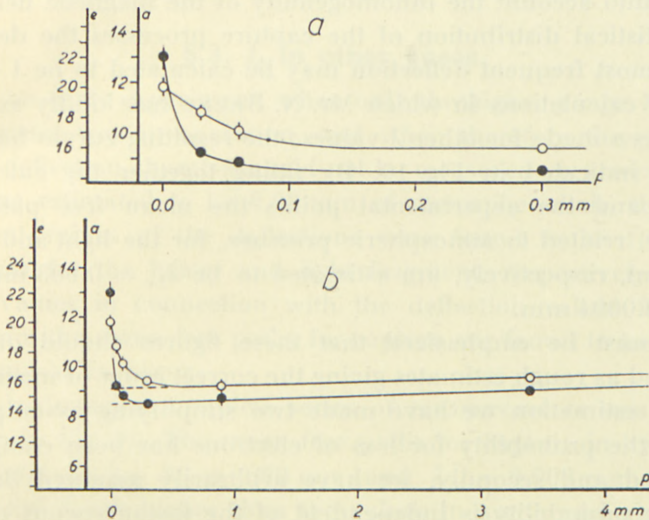


Fig. 10a and b. Most frequent deflection  $a$  in mm plotted against the pressure of argon in the deflection chamber. Open circles: Light fragment. Full circles: Heavy fragment.

per cent., which in the present connection may be neglected. The approximate scale of  $e$  is given to the left in the figure. As seen,  $e$  decreases from about  $21 \varepsilon$  for  $p = 0$  to about  $15 \varepsilon$  for  $p \approx 0.5$  mm A and then remains nearly constant; the increase of the ordinates of the curves for increasing  $p$ -values will be discussed later.

## § 2. Mean free path $\lambda_e$ for electron capture in argon.

From the curves in Fig. 10 we can roughly estimate the effective cross-sections for electron capture  $\sigma_e$  for the two fragments. At zero pressure the charges are determined by equilibrium between capture and loss of electrons in the passage of the fragments through the uranium layer. At a pressure of about 0.5 mm or higher the charges are determined by the equilibrium in the

gas. At the intermediate pressures the rate of decrease of the deflection is determined by the rate, with which the charges are changed due to capture of electrons in the gas. Suppose the pressure is increased from zero to such a magnitude that the mean free path  $\lambda$  for capture is, for instance, 50 mm; then, taking into account the inhomogeneity of the magnetic field and the statistical distribution of the capture processes the decrease of the most frequent deflection may be calculated to be 1.4 mm. Similar calculations in which Mr. N. BRENE has kindly assisted, have been made for other  $\lambda$ -values; the resulting curves have the shapes indicated in Fig. 10. By fitting together the calculated curves and the experimental points the mean free paths for capture, related to atmospheric pressure, for the light and heavy fragment, respectively, are estimated to be  $\lambda_{1c} = 0.003$  mm and  $\lambda_{2c} = 0.0004$  mm.

It must be emphasized that these figures should only be regarded as rough estimates giving the correct order of magnitude. By the estimation we have made two simplifying assumptions; firstly, the probability for loss of electrons has been completely neglected and secondly, we have arbitrarily assumed that the capture probability is independent of the instantaneous charge. From the charge distribution curve in Fig. 4 charge values more than  $5 \varepsilon$  higher than the equilibrium charge are seen to be rare; hence it must necessarily be deduced that for such highly charged fragments  $\sigma_c \gg \sigma_l$ . In the equilibrium the cross-sections for capture and loss are equal, and for all charge values in question we therefore have  $\sigma_c > \sigma_l$ . In view of the large difference between the starting values of the charges and the equilibrium charges it may be justified in the first approximation to neglect  $\sigma_l$  when calculating the beginning of the curves in Fig. 10.

The values of  $\lambda_c$  given above correspond to cross-sections of the order of magnitude  $10^{-16}$  cm<sup>2</sup>, which agree with theoretical estimates given by BOHR<sup>(6)</sup>. It may also be remarked that the heavy fragments has much the highest cross-section, which is in accordance with the smaller velocity. As a curiosity may be mentioned that we find  $\frac{\lambda_{2c}}{\lambda_{1c}} = \left(\frac{v_2}{v_1}\right)^{5.6} = 0.13$ , and that for  $\alpha$ -particles RUTHERFORD<sup>(8)</sup> has shown that  $\lambda_c$  is just proportional to  $v^{5.6}$  in the velocity range considered; however, from a theo-

retical point of view we have no reason to expect the same law to hold for fission fragments and, since the assumptions mentioned above might give different orders of approximation for the two fragments, the value found for  $\frac{\lambda_{2c}}{\lambda_{1c}}$  cannot claim any great accuracy<sup>1</sup>.

### § 3. $\lambda_c$ in other gases.

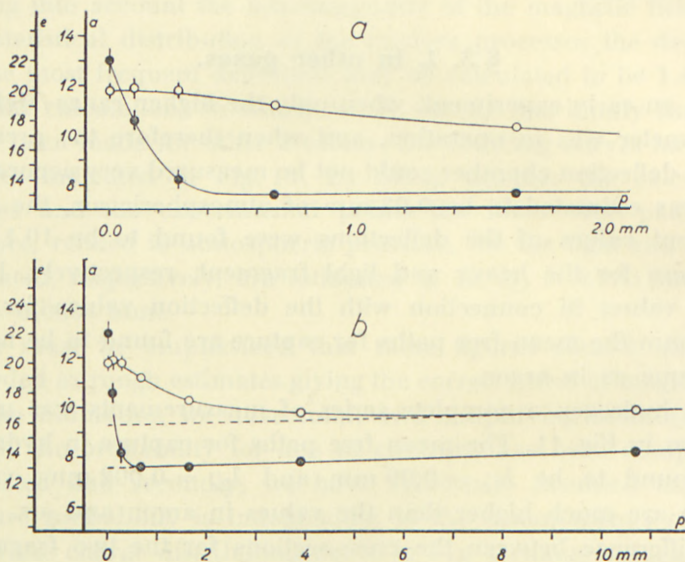
In an early experiment, when only the higher range McLeod manometer was in operation, and when therefore the pressure in the deflection chamber could not be measured very accurately, but was estimated to be 0.02 mm of atmospheric air, the most frequent values of the deflections were found to be 10.1 and 11.3 mm for the heavy and light fragment, respectively. From these values in connection with the deflection values for  $p = 10^{-3}$  mm the mean free paths for capture are found to be nearly the same as in argon.

In hydrogen a complete series of measurements was made, as seen in Fig. 11. The mean free paths for capture in hydrogen are found to be  $\lambda_{1c} = 0.09$  mm and  $\lambda_{2c} = 0.002$  mm, values which are much higher than the values in argon and air. Also, the difference between the cross-sections for the two fragments is much greater in hydrogen than in the heavier gases; the ratio  $\frac{\lambda_{2c}}{\lambda_{1c}}$  is in hydrogen found to be 0.02 as compared with the value 0.13 in argon, and although both ratios may be considerably in error, the great difference may indicate a stronger velocity dependence of the capture cross-section in hydrogen than in argon.

Since the cross-sections in hydrogen are so much smaller than those in heavier substances, it is obvious that the purity of the hydrogen plays a very great role. If the hydrogen gas contains 3 per cent. air one would get the above value of  $\lambda_{1c}$  even if the capture cross-section in hydrogen was vanishingly small; 20 per cent. air would be required to account for the observed value of  $\lambda_{2c}$ . The hydrogen was taken from a steel tank, which according to the manufactory contained hydrogen of a purity higher than

<sup>1</sup> A closer theoretical treatment of the capture and loss phenomena including also a more accurate estimate of the cross-sections for the processes will be given in a forthcoming paper by N. BOHR and J. LINDHARD in the "Mat. Fys. Medd." of the Royal Danish Academy of Sciences and Letters, Copenhagen.

99.9 per cent. Before each experiment the deflection chamber was thoroughly exhausted and filled with the gas at least three times. At the beginning of the experiment the gas may therefore be expected to contain less than 0.1 per cent. impurities. During the working time of about 5 hours the pressure rise of the im-



Figs. 11a and b. Most frequent deflection  $a$  in mm plotted against the pressure of hydrogen in the deflection chamber.

purities may amount to 0.005 mm. Thus for the pressure  $p = 1.65$  mm, which is significant for the determination of  $\lambda_{1e}$  the impurities at the end of the experiment should be smaller than 0.4 per cent., and consequently the influence of the impurities on the value of  $\lambda_{1e}$  is negligible. For  $p = 0.28$  mm, a pressure which is of importance for the determination of  $\lambda_{2e}$  we must expect the impurities at the end of the experiment to be smaller than 2 per cent.; also in this case the influence of the impurities is negligible.

In helium no direct measurements of the mean free paths have been carried out. The deflections have only been measured for relatively high pressures (2 mm and higher), but from these measurements it is indicated, in qualitative accordance with theory, that  $\lambda_{1e}$  is smaller than in hydrogen by at least a factor of 2 or 3.



#### § 4. The equilibrium charges in gases at low pressure.

Since the curves in Fig. 10b for higher  $p$ -values are not exactly horizontal, the minima on the curves may be taken to represent the equilibrium charges at the lowest pressures. In the present treatment it has, however, been chosen to extrapolate the linear parts of the curves backward to intersection with the axis  $p = 0$  and to define the equilibrium charges corresponding to zero pressure as the ordinates of the intersection points. The

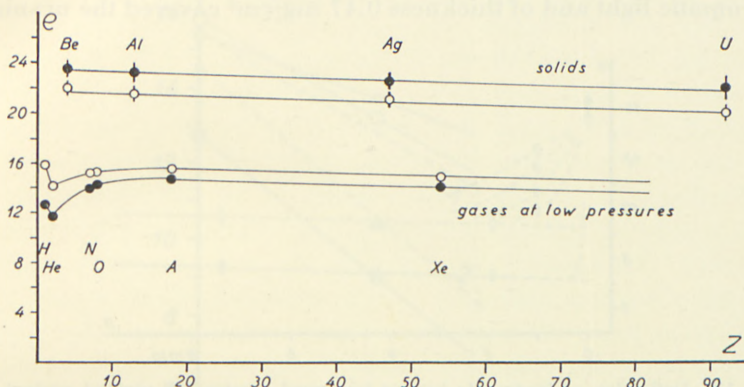


Fig. 12. The equilibrium charges in various substances plotted against the nuclear charge of the stopping atoms.

difference between the values so defined and the minimum values is quite small in all cases except one, the charge of the light fragment in hydrogen. In this case the difference becomes larger, because a rather high pressure is needed to give "equilibrium"; the extrapolation is shown in Fig. 11 and in Fig. 17.

Fig. 12 gives the equilibrium charges in various gases (the two lower curves). Leaving hydrogen out of account  $e$  seems to increase with  $z$  for small atomic numbers; it reaches a maximum for argon and decreases slightly for higher  $z$ -values. The points for  $H_2$  lie considerably higher than would be expected from an extrapolation of the rest of the curves; thus, although the charges in  $H_2$  are not much higher than in the heavy gases,  $e_2$  on the contrary being lower than in most of the gases, they may in a certain sense be said to be rather high. For both fragments the charge is considerably higher in  $H_2$  than in He.

It is satisfactory that the difference  $e_1 - e_2$  is higher in  $H_2$  than in A, because it is in accordance with the results for the effective charges already referred to<sup>(3)</sup>. It is also in conformity with the larger relative difference between  $\lambda_{1c}$  and  $\lambda_{2c}$  in hydrogen.

### § 5. The variation of the charges along the path.

In Fig. 13 is shown the result of some measurements in  $H_2$ , in which a mica foil tested for homogeneity by means of monochromatic light and of thickness  $0.47 \text{ mg/cm}^2$  covered the uranium

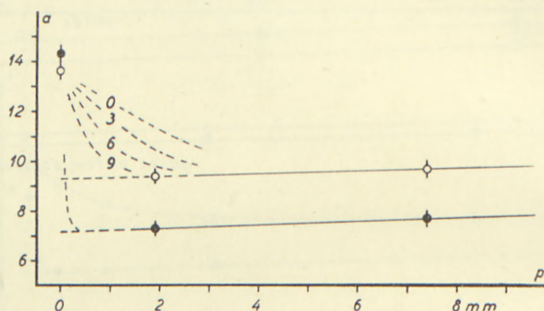


Fig. 13. Deflection of fragments having traversed a mica foil plotted against the pressure of hydrogen in the deflection chamber.

layer. The ordinate is the deflection  $\alpha$ , which is proportional to  $\frac{e}{mv}$ , but here  $mv$  is not the same for the two fragments, since they have been slowed down in unequal ratios. As the fragments traverse the mica foil in a direction making an angle of nearly  $45^\circ$  with the normal, the effective thickness is  $0.66 \text{ mg/cm}^2$ , which according to the previous paper<sup>(3)</sup> corresponds to  $0.47 \text{ cm}$  of argon. Using the range velocity relation given in the mentioned paper it is found that  $v'_1 = 0.83 \cdot v_1$  and  $v'_2 = 0.73 \cdot v_2$ ,  $v'_1$  and  $v'_2$  being the velocities of the fragments having passed the mica foil, and  $v_1$  and  $v_2$  being the initial velocities. Using these values one gets from Fig. 13 for the equilibrium charges  $e'_1 = 13.2 \varepsilon$  and  $e'_2 = 9.0 \varepsilon$ . The charges at the surface of the mica foil are  $18.8 \varepsilon$  and  $17.2 \varepsilon$  for the light and heavy fragment, respectively.

Since the two curves in Fig. 13 are parallel down to a pressure of 2 mm, while the corresponding curves in Fig. 11 b are only

parallel down to about 6 mm it is seen that the rate of decrease of the deflection of the light fragment is the higher for the slower fragments, e. g. that  $\lambda'_{1c}$  corresponding to the velocity  $v'_1$  is smaller than  $\lambda_{1c}$  corresponding to the initial velocity, a result, which should also be expected. An attempt to estimate the ratio  $\frac{\lambda'_{1c}}{\lambda_{1c}}$  has been made by means of the curves denoted 0, 3, 6, and 9,

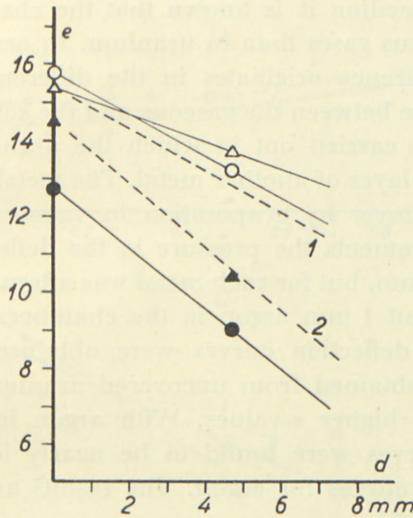


Fig. 14. The charges in H<sub>2</sub> and A as functions of the path *d* traversed. Circles and triangles correspond to H<sub>2</sub> and A, respectively. *d* is given in mm of argon.

where for instance curve 3 corresponds to a value  $\lambda'_{1c} = \lambda_{1c} \cdot \left(\frac{v'_1}{v_1}\right)^3$ . As seen, the  $\lambda$ -values determined on the previously mentioned basis seem to vary with a high power of the velocity.

Similar measurements in argon indicate that also in this gas  $\lambda'_{1c}$  for fragments having passed the mica foil is smaller than the initial value. The equilibrium charges are found to be  $e'_1 = 13.7 \varepsilon$  and  $e'_2 = 10.4 \varepsilon$ .

In Fig. 14 the charges in hydrogen and argon are plotted against the path *d* traversed by the fragments; *d* is given in mm of argon. The dotted lines 1 and 2 are drawn proportional to  $v_1$  and  $v_2$ , respectively, and, as seen, the charges vary nearly

proportional to  $v$  in agreement with theory<sup>(6)</sup>. In fact, the relation  $e \propto v$  holds within the limits of error except for the light fragment in argon, which shows a slightly more slowly variation of  $e$ .

### Chapter III. The Charges in Solid Materials.

From the preceding it is known that the charges are much lower in the various gases than in uranium. In order to examine whether this difference originates in the difference in  $z$ -values or in the difference between the gaseous and the solid states, some experiments were carried out in which the uranium layer was covered by a thin layer of another metal. The metal was deposited on the uranium layer by evaporation in vacuo. By the actual deflection measurements the pressure in the deflection chamber was kept at  $10^{-3}$  mm, but for each metal was afterwards measured a curve with about 1 mm argon in the chamber. With vacuum in the chamber deflection curves were obtained, which were similar to those obtained from uncovered uranium, but slightly displaced against higher  $e$ -values. With argon in the chamber the deflection curves were found to be nearly identical to the earlier measured curves for argon. The results are summarized in Table 1.

Neglecting the decrease of velocity in the covering media the

TABLE 1.

covering medium	thickness <sup>1</sup> in mg/cm <sup>2</sup>	Most frequent deflections			
		In vacuum		1 mm argon	
		a <sub>1</sub>	a <sub>2</sub>	a <sub>1</sub>	a <sub>2</sub>
Be	0.13	13.0 ± 0.3	13.9 ± 0.3	9.5 ± 0.3	8.8 ± 0.3
Al	0.07	12.7 ± 0.3	14.0 ± 0.5	9.5 ± 0.3	8.7 ± 0.3
Ag	0.18	12.2 ± 0.3	13.1 ± 0.3	9.5 ± 0.4	8.7 ± 0.4
none	0	11.8 ± 0.3	13.0 ± 0.5	9.2 ± 0.3	8.7 ± 0.3
none	0	11.6 ± 0.6	12.9 ± 0.6	..	..
none <sup>2</sup>	0	11.8 ± 0.3	12.6 ± 0.4	9.3 ± 0.3	8.8 ± 0.3

<sup>1</sup> The fragments traverse the layer obliquely.

<sup>2</sup> Another geometry.

most frequent charges given in Fig. 12 are obtained. They are seen to be markedly higher in the lighter substances than in uranium.

However, a priori a slight possibility might exist that the higher deflections for the lighter materials were caused by the slowing down of the fragments, since nothing was known with certainty about the variation of  $\frac{e}{mv}$  along the path in these materials. In order to exclude this possibility a series of measure-

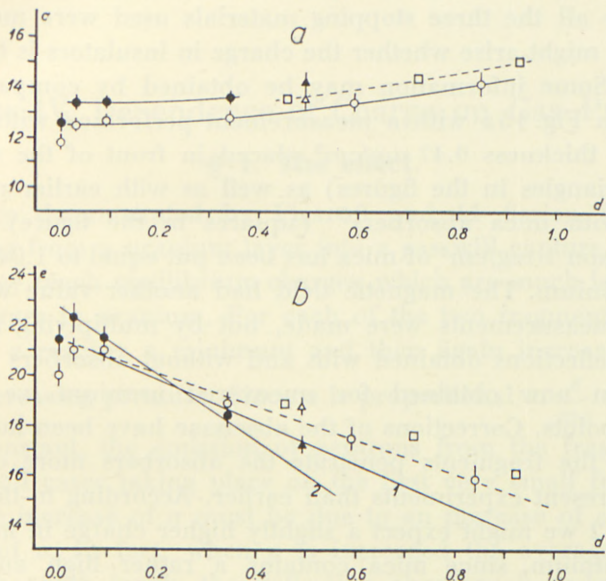


Fig. 15a. Deflections of fragments in aluminium as functions of the thickness of the aluminium absorber.

Fig. 15b. The charges in aluminium as functions of the thickness of the aluminium absorber.

The fragments traverse the absorber obliquely. The abscissae correspond approximately to the path traversed measured in mm of argon. Squares and triangles refer to mica, see text.

ments was performed with aluminium absorbers of various thicknesses. In this series the geometry was slightly altered; the widths of uranium layer and slit were 1.0 mm, that of the window 3.0 mm. The two thinnest aluminium absorbers were made by successive evaporation in vacuo; the other absorber thicknesses were obtained by additional aluminium foils. The result is shown in Fig. 15a from which it is seen beyond any doubt, that the charges are higher in Al than in U.

In argon at a pressure of 0.5 mm the equilibrium charge will be reached on a path of the order of magnitude 1 cm, as may be deduced from Fig. 10. In respect to velocity decrease this length corresponds to about  $0.001 \text{ mg/cm}^2$  Al. Hence it may be expected that equilibrium is reached for much thinner layers than those used here; in view of this and of the rather small difference in charge no attempt was made to determine  $\lambda_t$ .

Since all the three stopping materials used were metals the question might arise whether the charge in insulators is the same or not. Some information may be obtained by comparing the curves in Fig. 15a with a measurement performed with a mica sheet of thickness  $0.47 \text{ mg/cm}^2$  placed in front of the uranium layer (triangles in the figures) as well as with earlier measurements with mica absorbers<sup>(9)</sup> (squares in the figure). By this comparison  $1 \text{ mg/cm}^2$  of mica has been put equal to  $1.04 \text{ mg/cm}^2$  of aluminium. The magnetic field had another value when the earlier measurements were made, but by multiplying the ratio of the deflections obtained with and without absorbers with the deflection now obtained for uncovered uranium we get the square points. Corrections of the abscissae have been introduced because the fragments penetrate the absorbers more obliquely in the present experiments than earlier. According to the curves in Fig. 12 we might expect a slightly higher charge in mica than in aluminium, since mica contains a rather high amount of oxygen. As seen, the points in Fig. 15a agree with this expectation, and although we cannot with certainty deduce, that the initial charges in mica fit with the curves in Fig. 12 it is rather likely to assume so. At least it is a fact, that fragments with velocities about 80 per cent. of the initial velocities have almost the same charges in mica as in light metals.

Thus there is a large difference between the charges of fission fragments in gaseous and solid stopping media, but none or almost none between the charges in metals and insulators.

If the charges had decreased along the range proportional to  $v$  the deflections would have been independent of the absorber thicknesses. Fig. 15a therefore shows that the decrease is slightly more slowly, at least for the light fragment. The same is seen from Fig. 15b, which gives directly the charges as functions of

the path traversed; there the ordinates of the fulldrawn curves 1 and 2 are proportional to  $v_1$  and  $v_2$ , respectively.

As seen, the curves for the two fragments intersect each other. At the initial velocities the heavy fragment has the higher charge, but after some slowing down the charges of the two fragments become equal (for a velocity ratio  $v_2 : v_1 = 0.66$ ); after further stopping the light fragment will have the higher charge equal to what is the case along the whole path in gaseous stopping media.

## Chapter IV. Dependence of Charge on Gas Pressure.

### § 1. The effect.

As is demonstrated by Figs. 10 and 11 fission fragments emerging from a uranium layer into a gas will capture electrons until they reach equilibrium charges, which are much lower than the charges in uranium. For each of the two fragments the deflection  $a$  reaches a minimum and then again increases slowly with increasing pressure. Since  $a$  is proportional to  $\frac{e}{mv}$  and since  $m$  is constant, the emission of neutrons from the fragments in almost all cases taking place on the first very small fraction of a  $\mu$ , the increase of  $a$  must be due to an increase of  $e$  or a decrease of  $v$ . In fact, when  $p$  is increased the average velocity along the path inside the deflection chamber is reduced and, of course, at first the increase of  $a$  was considered to be a result of this velocity decrease. However, a closer consideration shows that this explanation is insufficient. Looking at the curve for the heavy fragment, for instance, we find an increase in  $a$  of 5 per cent. when  $p$  is increased from 0 to 3 mm argon; the average velocity is 2.2 per cent. lower for  $p = 3$  mm argon than for  $p = 0$ , as may be calculated from the dimensions of the apparatus and the range velocity relation. Thus, even if the charge  $e_2$  were constant along the path, the velocity decrease is insufficient to account for the observed increase of the deflection. Moreover, from the previous it is known that  $e_2$  varies nearly proportional to  $v_2$ . Hence, the slowing down of the fragments will cause no increase at all in  $a$ , and  $\frac{e}{mv}$  will be constant along the path from

the point where the equilibrium charge is reached. (Of course, we are here speaking about mean values of the charge, and the fluctuations are not considered.)

Although an increase in  $a$  of 5 per cent. is not very much higher than the uncertainty the increase must be considered as an experimental fact, in view of the circumstance, that a corresponding increase is found for both fragments in  $H_2$ , He,  $O_2$ , A and Xe, and in case of  $H_2$  and A also for smaller velocities.

The dependence of the mean charge of the fragment ions on the gas pressure can be accounted for in the following way. After a collision with a gas atom the fragment may be left in an excited state. If the density of the gas is high, so that the time intervals between successive collisions are short, the ion may still remain in the excited state when the next collision takes place. However, if the next collision occurs after the lapse of a sufficiently long time, the ion will have reached its ground state by a radiative transition, and this leads to a reduced effective cross-section for loss. Hence, for low pressures the ion is expected to carry more electrons.

At a pressure of 3 mm argon the increase of the charge amounts to about one unit. At this pressure the time interval between successive interchanges of charge is of the order of magnitude  $\frac{\lambda}{v} \sim 10^{-11}$  sec. This may give a hint when estimating the magnitude of the life times of the excited states in question.

## § 2. The charges at higher pressures.

A priori very little can be said about the charges at higher pressures, although it is obvious that the rate of increase must become smaller with increasing pressure. In order to attempt an experimental investigation measurements were carried out for increasing values of  $p$  up to such a limit that for higher pressures the residual energy of fragments reaching the ionization chamber would be too small. The resulting curves are shown in Figs. 16 and 17. It must, however, be noticed that to get the charges corrections must be introduced, since for higher pressures it is necessary to take into account the variation of  $v$  and the deviation from proportionality between  $e$  and  $v$ . This fact together with



the rather small variation in  $a$ , as compared with the uncertainty, make the discussion of the curves somewhat complicated.

Knowledge about the variation of  $\frac{e}{mv}$  with the velocity may be obtained from the measurements with a mica absorber already mentioned; the  $a$ -values obtained in these experiments by the usual extrapolation to zero pressure are summarized in Table 2.

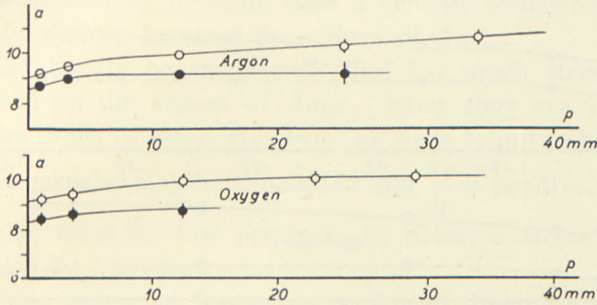


Fig. 16. Deflection vs. pressure in argon and oxygen.

Though the variations of  $\frac{e}{mv}$  do not amount to more than a few per cent., they are high enough to be importance. As seen, the influence will be, just in accordance with the curves in Figs. 16 and 17, to increase the  $a$ -values less for the heavy fragment than for the light fragment, even when  $e$  did not depend on  $p$ . A closer consideration shows that in  $H_2$  as well as in A  $e_1$  and  $e_2$  are both found to increase with  $p$  also for the higher pressures; the increase of  $e_1$  is in both gases found to be slightly higher than the increase of  $e_2$ , but the difference is smaller than the uncertainty.

TABLE 2.

	Light fragment						Heavy fragment					
	without absorber		with absorber		$\Delta a_v$ %	$\Delta v$ %	without absorber		with absorber		$\Delta a_v$ %	$\Delta v$ %
	$a$ mm	$v$ %	$a$ mm	$v$ %			$a$ mm	$v$ %	$a$ mm	$v$ %		
$H_2$	9.3	100	9.3	83	0	17	7.5	100	7.1	73	-5	27
A	9.0	100	9.6	83	7	17	8.5	100	8.3	73	-2	27

The values of  $a$  and therefore of  $\Delta a_v$  in Table 2 refer to  $p = 0$ .  $\Delta a_v$  might have other values at higher pressures, and therefore further measurements were carried out with the mica absorber and with rather high pressures. The results of these experiments as well as of some of those from Figs. 16 and 17 are given in Table 3. Here  $\Delta a$  denotes the increase of  $a$  (in per cent.) which is obtained when  $p$  is increased from 32 to 95 mm of  $H_2$ , or corresponding values of the other gases, and

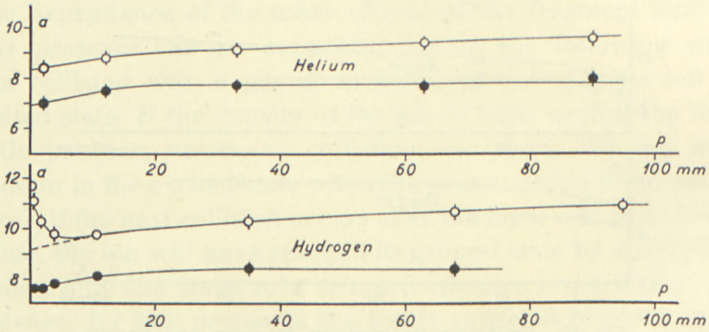


Fig. 17. Deflection vs. pressure in helium and hydrogen.

$\Delta v$  is the corresponding decrease of the mean velocity in the deflection chamber.  $\Delta a_v$  is the increase of  $a$  when the mica absorber is interposed, and  $\Delta v'$  is the decrease of the mean

TABLE 3.

	$p$ mm	without absorber						with absorber				$\Delta a_v$ %	$\Delta v'$ %	$\Delta a_{\text{korr}}$ %
		velocity %			$a$ mm	$\Delta a$ %	$\Delta v$ %	velocity %			$a$ mm			
		start	mean	end				start	mean	end				
$H_2$	32.4	100	94	89	10.2	..	..	83	75	67	10.0	-2	19	..
	95	100	80	60	10.9	7	14	..	..	..	..	..	..	8
He	28.5	100	..	..	9.1	..	..	83	..	..	9.0	-1	..	..
	90	100	..	..	9.6	5	..	..	..	..	..	..	..	5
$O_2$	12.9	100	94	87	9.9	..	..	83	76	68	9.9	0	18	..
	29	100	85	70	10.1	2	9	..	..	..	..	..	..	2
A	12.5	100	94	88	10.0	..	..	83	76	69	10.6	6	18	..
	34	100	83	66	10.7	7	11	..	..	..	..	..	..	3

velocity in the chamber caused by the absorber,  $\Delta a_{\text{kor}}^{\text{r}}$  is determined as  $\Delta a - \Delta a_v \cdot \frac{\Delta v}{\Delta v'}$ , and should be that part of  $\Delta a$  which is caused by the increase of  $e$  with pressure, thus  $\Delta a_{\text{kor}}^{\text{r}} \text{ } ^0/0 = \Delta e \text{ } ^0/0$ . The mean value of  $v$  equals the velocity at the mid-point of the path in the deflection chamber; since the magnetic field is about 2.5 times higher at the beginning than at the end of the path inside the chamber, it might be more correct in stead of the mean velocity to count with a velocity somewhat higher; this would slightly increase the values of  $\Delta a_{\text{kor}}^{\text{r}}$ .

It need hardly be mentioned, that too much stress should not be laid on the values of  $\Delta a_{\text{kor}}^{\text{r}}$ , since they are not much outside the limits of error. However, as  $\Delta e$  is found to be positive in all four gases, it may be concluded that  $\frac{\partial e}{\partial p}$  is positive, although it is smaller than for low pressures by about a factor of 10 as should also be expected.

The light group of fragments is slowed down by the same amount in argon at a pressure  $p$  as in hydrogen at the pressure  $3 p$ . If the pressure in the various gases is measured in corresponding units, defined as such pressures giving equal stopping power,  $\frac{\partial e}{\partial p}$  is, at high pressures, found to be higher for the light than for the heavy gases. At low pressures, however,  $\frac{\partial e}{\partial p}$  is in all gases nearly the same, when  $p$  is measured in such units.

When the pressure of argon is increased from 0 to about 10 mm  $e_1$  increases from 15.5  $\varepsilon$  to 17  $\varepsilon$ , and  $e_2$  with a similar amount. From the mentioned measurements at higher pressure can only be deduced that the rate of increase of  $e$  is smaller at higher pressures. It may be that the charge becomes practically constant for  $p = 10$  mm. If this is the case the total charge will be lower than the effective charge determined from ionization measurements at about 150–300 mm A<sup>(3)</sup>. However, if the increase of 3 per cent. for a pressure increase of 20 mm is real, and if  $\frac{\partial e}{\partial p}$  goes but slowly against zero, the charges may reach values equal to those previously obtained for the effective charges.

It would be of high interest to investigate the charge dependence on pressure for higher  $p$  values than used in the present experiments. Therefore a new deflection apparatus with a considerably shorter deflection chamber is under construction. It is also planned to examine whether the effective charges vary with  $p$ , e. g. whether the specific ionization by fission fragments relative to that by  $\alpha$ -particles is a function of the pressure.

The present experiments were carried out at the Institute for Theoretical Physics in Copenhagen, and the author wishes to express his heartiest thanks to the Director of the Institute, Professor NIELS BOHR, for his great and continued interest in the work. Furthermore, my thanks are due to Professor J. C. JACOBSEN for helpful advice in experiments and to Mr. J. LINDHARD for valuable discussions.

*Institute for Theoretical Physics,  
University of Copenhagen,  
Denmark.*

---

### References.

1. N. O. LASSEN: Dan. Mat. Fys. Medd. **23**, no. 2, 1945.
2. — Phys. Rev. **68**, 142, 1945.
3. — Dan. Mat. Fys. Medd. **25**, no. 11, 1949.
4. — Phys. Rev. **70**, 577, 1946.
5. — Phys. Rev. **75**, 1762, 1949.
6. N. BOHR: Dan. Mat. Fys. Medd. **18**, no. 8, 1948.
7. N. O. LASSEN: Phys. Rev. **79**, 1016, 1950.
8. RUTHERFORD: Phil. Mag. **47**, 277, 1924.
9. N. O. LASSEN: Phys. Rev. **69**, 137, 1946.